ORIGINAL ARTICLE

Renal responses produced by microinjection of the kappa opioid receptor agonist, U50-488H, into sites within the rat lamina terminalis

Cynthia Franklin[1], Lourdes Fortepiani[2], Tin Nguyen[1], Yolanda Rangel[3], Randy Strong[4] & Helmut B. Gottlieb[1],

[1]Department of Pharmaceutical Sciences, Feik School of Pharmacy, University of Incarnate Word, San Antonio, Texas, 78209
[2]Rosenberg School of Optometry, University of Incarnate Word, San Antonio, Texas, 78209
[3]Department of Physical Therapy, University of Texas Health Science Center at San Antonio, San Antonio, Texas, 78229
[4]Department of Pharmacology and the Barshop Institute for Longevity and Aging Studies, University of Texas Health Science Center at San Antonio and the SouthTexas Veterans Health Care System, San Antonio, Texas, 78229

Abstract

Activation of central kappa opioid receptors (KOR) has been demonstrated to produce marked free water diuresis with a concurrent increase in renal sympathetic nerve activity (RSNA). This study investigated the cardiovascular (CV) and renal effects evoked by central activation of KOR in two lamina terminalis sites, the median preoptic area (MPA) and anterolateral division of the bed nuclei of the stria terminalis (BST). Rats anesthetized with urethane alpha-chloralose were instrumented to record mean arterial pressure, heart rate, RSNA, and urine output (V). Rats were infused with isotonic saline (25 μL/min) and urine samples were collected during two 10-min control periods and six consecutive 10-min experimental periods following microinjection of vehicle, U50-448H (U50, KOR agonist) alone or norbinaltorphimine (nor-BNI, KOR antagonist) plus U50. Microinjection of U50 into the BST increased V (peak at 30 min, 84.8 ± 12.9 μL/min) as compared to its respective control, vehicle, or nor-BNI plus U50. This diuretic effect occurred without any significant changes in CV parameters, RSNA, or urinary sodium excretion. In contrast, U50 injection into the MPA significantly increased RSNA (peak at 20 mins: 129 ± 9.9) without increasing the other parameters. This study demonstrated novel sites through which activation of KOR selectively increases V and RSNA. The ability of U50 to increase V without affecting sodium excretion and RSNA raises the possibility that LT neurons could be an important substrate through which drugs targeting KOR could selectively facilitate water excretion in sodium-retaining diseases such as congestive heart failure.

Abbreviations
BST, bed nuclei of the stria terminalis; ICV, intracerebroventricular; KOR, kappa opioid receptor; MPA, median preoptic area; nor-BNI, norbinaltorphimine; RSNA, renal sympathetic nerve activity; U50, U50488H; UNaV, sodium excretion rate; V, urine output.

Introduction

Central administration of kappa opioid agonists, for example, U-50448H (U50), produces a marked diuresis, antinatriuresis, and an increase in renal sympathetic nerve activity (RSNA) in conscious and anesthetized rats (Leander et al. 1987; Oiso et al. 1988; Kapusta and Obih 1993; Kapusta 1995; Gottlieb et al. 2005b). Although a number of studies suggest that the kappa opioid-mediated diuretic effect results from central inhibition of

hypothalamic magnocellular neurons involved in the secretion of arginine vasopressin (AVP) (Oiso et al. 1988; Brooks et al. 1993; Brown et al. 1998, 1999; Gottlieb et al. 2005b), the exact mechanism and sites are yet to be fully understood. Furthermore, the central nervous system (CNS) sites involved in the antinatriuretic and the increases in RSNA remain unknown. Kapusta and Obih (1993) proposed that the central antinatriuretic effect of kappa opioid agonists are dependent on intact renal nerves since bilateral renal denervation abolished the kappa-mediated decrease in sodium excretion without affecting glomerular filtration rate and effective renal plasma flows.

Sly et al. (1999) identified various forebrain regions, via pseudorabies virus injection into the kidney and retrogradely traced back to CNS sites that may be involved in the sympathetic modulation of renal nerves and consequent antinatriuretic effect. The lamina terminalis (LT), formally known as the anteroventral region of the third ventricle (AV3V), is a region of interest since it not only contains neuronal projections to the kidneys but has also been shown to be involved in the maintenance of water, electrolytes, and cardiovascular (CV) function (Bealer and Johnson 1979; Brody and Johnson 1980; McKinley et al. 1992, 2001, 2004). The LT has also been implicated in the control of these physiological functions at least, in part, through GABAergic and glutamatergic projections to the paraventricular nucleus of the hypothalamus (PVN) (Boudaba et al. 1996; Grob et al. 2003; Llewellyn et al. 2012). The PVN is a major CNS site involved in the control of sympathetic nervous system and fluid and electrolyte homeostasis, and integrates inputs from other regions (Sawchenko and Swanson 1983; Roland and Sawchenko 1993; Zardetto-Smith et al. 1993; Grob et al. 2003). Kappa opioid receptors (KOR) have been shown to be present in the PVN and LT, and activation of these receptors within the PVN and supraoptic nucleus (SON) has been show to inhibit magnocellular neurons firing (Conway et al. 1987; Mansour et al. 1994, 1996; Brown et al. 1998, 2000, 2006; Gottlieb et al. 2005b). Thus, inhibition of AVP secretion has been proposed to be one of the mechanism via which kappa agonists evoke at least in part their diuretic effect.

The PVN receives projections from a number of sites within the LT, which includes the median preoptic area (MPA) and anterolateral division of bed nuclei of the stria terminalis (BST) (Kawano and Masuko 2000; Dong and Swanson 2006a). The MPA has been implicated in thermoregulation, endocrine, and CV function (Diez-Guerra et al. 1987; Hunt et al. 2010; Morrison 2011). The MPA also receives projections from the arcuate nucleus, a site known to be involved in the production of the endogenous kappa opioid agonist dynorphin (Maolood

and Meister 2008), and has been shown to send inhibitory projections to both magnocellular and parvocellular neurons in the PVN (Boudaba et al. 1996). Another site of interest within the LT region is the anterior division of bed of the stria terminalis (BST), which has been further subdivided into two major regions, anteromedial and anterolateral groups(Dong et al. 2001). Both sites receive projections from other forebrain and hindbrain regions involved in autonomic function (Dong and Swanson 2006a,b; Gaykema et al. 2007). The BST and MPA efferent synapses with forebrain regions involved in autonomic nervous system, for example, PVN, and have been shown to express KOR (Dong and Swanson 2006a,b; Poulin et al. 2009; Hunt et al. 2010). As such, we hypothesize that activation of KOR in the anterolateral regions of the BST and the MPA would evoke similar changes to urinary flow rate, sodium excretion rate, and RSNA as observed with intracerebroventricular (ICV) injection of KOR agonists.

The purpose of this study was to investigate the CV and renal effects evoked by microinjection of a selective kappa opioid agonist into two discreet LT sites, the MPA, and anterolateral BST. This study provides insights in the possible CNS sites involved in the diuretic and renal sympathoexcitatory effects mediated by KOR activation.

Materials and Methods

Subjects

Experiments were performed using male Sprague–Dawley rats (300–350 g Harlan, Indianapolis, IN). The rats were housed in a temperature- and humidity-controlled room with a 12-h light/dark cycle. Standard rat chow and tap water were available at will. All procedures using animals were conducted according to the NIH guidelines, and were reviewed and approved by the Institutional Animal Care and Use Committees at University of Texas Health Science Center at San Antonio and University of Texas San Antonio.

Surgical and experimental procedures

On the day of the experiment, rats were anesthetized with isoflurane (2–3% in oxygen) and catheters (polyethylene PE-50 tubing; Becton, Dickinson and Company, Franklin Lakes, NJ) were placed in a femoral artery and vein to measure arterial blood pressure, and for isotonic saline and drug infusion, respectively. Through a suprapubic incision, a catheter (flanged PE-240; Becton, Dickinson and Company) was also implanted into the urinary bladder for collection of the urine samples. All catheters were exteriorized and securely sutured to adjacent muscle and

skin. The arterial and venous catheters were connected to a pressure transducer and an infusion pump, respectively. The mean and pulsatile arterial pressures were measured using a LP122 AC/DC amplifier (Grass instruments, Quincy, MA). Blood pressure was recorded and integrated using a Micro-1401 data acquisition unit and Spike 7 software package (Cambridge Electronic Design, CED, Ltd., Cambridge, England). Heart rate (HR) was determined from the arterial pressure signal using the Spike 7 software.

Animals were also implanted with a recording electrode on a renal nerve bundle for direct measurement of multifiber RSNA using a Grass model LP122 AC/DC. The left kidney was exposed through a left incision via a retroperitoneal approach. With the use of a dissecting microscope (25X), a renal nerve branch from the aortic renal ganglion was isolated and carefully dissected. The renal nerve branch was then placed on a bipolar platinum wire electrode (A-M Systems Inc., Carlsborg, WA). RSNA was amplified (10,000–50,000X) and filtered (Low, 30 HZ; High 300 Hz) with a Grass P511 band-pass amplifier. When an optimal RSNA signal was observed, the recording electrode was fixed to the renal nerve branch with dental impression material (Coltene President, Coltene/Whaledent Inc., NJ). The electrode cable was secured in position by a suture to the abdominal trunk muscle. Then, the electrode cable was exposed and the flank incision was closed. The integrated voltage signals were displayed on the Micro-1401CED system through the Spike 7 software. Integrated RSNA was expressed as microvolt-seconds per 1-sec interval. For each 10-min control and experimental periods, the values for integrated RSNA were sampled over the entire collection period and the numbers were averaged. RSNA was expressed as the percentage of baseline value obtained during the control period, with this being expressed as 100% for each animal. We determined the background noise of RSNA by observing the neural signal that remained 10 min after the end of the experiment by injecting hexamethonium (30 mg/kg, i.v.), a ganglionic blocker.

After implantation of catheters and a renal nerve recording electrode, rats were removed from the isoflurane and anesthesia was maintained with a mixture of alpha-chloralose (80 mg/kg i.v.) and urethane (800 mg/kg i.v.). An adequate depth of anesthetic was assessed by the absence of limb withdrawal or pressure response to the foot pinch. Supplemental anesthetic (10%) of initial dose was given as necessary. Rats were placed prone in a stereotaxic apparatus with the bite bar 3.5 mm below the interaural line. A craniotomy was performed above the site of the MPA or BST. Drugs or vehicle was microinjected unilaterally into the desired site using a three-barrel glass micropipette (0.4 mm I.D., 0.75 mm O.D.) with a composite tip diameter of less than 40 μm. The coordinates for the microinjection of the drug/vehicle into the antero-lateral BST were 1.8 mm lateral to either side of the midline, and 6.6 mm below the surface of the skull. MPA coordinates were 0.6 mm lateral to either side of the midline, and 8.5 mm below the surface of the skull. Because both the BST and MPA encompass a large portion of the LT, we targeted 0.00 mm anterior/posterior to bregma with an accepted range between −0.12 and +0.12 mm. Brain coordinates were obtained from the atlas of Paxinos and Watson (2007). The barrels 1 and 2 of the pipettes were filled by vacuum with U50 (100 ng/60 nL) and nor-BNI (10 ng/60 nL). Barrel 3 was filled with red fluorescent beads (Red retrobeads, .2%, Luma Fluor Inc., Durham, NC) dissolved in isotonic saline vehicle (60 nL), which were used to mark the injection site. These fluorescence beads have no pharmacological activity and have been used in electrophysiology studies for juxtacellular labeling. The doses of U50 and nor-BNI microinjected were previously established (Gottlieb et al. 2005b) and compared to ICV injections from a previous study (Gottlieb et al. 2005b). All drugs and vehicle were injected in a volume of 60 nL over a period of 0.5–1 min. The speed and volume of the injection were controlled by watching the movement of the fluid meniscus in the pipette with a stereomicroscope and graticule affixed to the pipette.

Western blot analyses of brain kappa opioid receptor

Samples from the forebrain of normal naïve, healthy Sprague–Dawley (SD) ($n = 5$) control rats were analyzed using standard western blot techniques. Briefly, each rat was anesthetized with Inactin (100 mg/kg, i.p.) and decapitated. The extracted brain was placed in a commercially available brain matrix (Stoelting, Wood Dale, IL) and cut into 1-mm-thick coronal slabs with razor blades. Micropunched brain tissue samples from the stereotaxic coordinates corresponding to PVN, SON, anterior BST, dorsal BST, and MPA were obtained with a 1-mL syringe equipped with blunt sterile 23-gauge needle. The punched samples were expelled into microcentrifuge tubes and snap-frozen on dry ice. Tissue was sonicated in RIPA Buffer containing protease inhibitor cocktail (Sigma Aldrich, St. Louis, MN). Protein concentration was determined by the Bio-Rad protein assay based on the Bradford method (Bio-Rad, Hercules, CA). Brain nuclei homogenates (5 μg) were separated by SDS-PAGE. Proteins were then electrophoretically blotted onto polyvinylidene difluoride (PVDF) membranes. Membranes were probed with polyclonal anti-KOR receptor antibodies obtained from Pierce (Thermo Fisher Scientific, Rockford, IL). After they were washed, the PVDF membranes were incubated with

bovine anti-rabbit IgG secondary antibody conjugated with horseradish peroxidase (Cell signaling, Danvers, MA). Bands were detected by ECL Plus (Amersham, Pittsburgh, PA) and quantified by densitometry. Membranes were reprobed with anti-GAPDH antibody (Sigma-Aldrich) as a loading control. Blots were performed three times with brain nuclei tissue samples from three rats. KOR is widely expressed in the rat brain at different densities. Rat cerebellum tissue, where KOR expression has been previously described, was used as a positive control and rat liver tissue, which does not express KOR, was collected and run as a control for specificity of the antibody.

Experimental protocol

Under urethane/alpha-chloralose anesthesia, rats were continuously infused with isotonic saline (25 μL/min) for the entirety of the protocol, allowing 1–2 h for stabilization of CV and renal parameters. The glass micropipette was lowered into position following the coordinates previously described and two consecutive 10-min control urine samples were collected. U50 (100 ng/60 nL), isotonic saline vehicle, nor-BNI alone (10 ng/60 nL; data not shown), or nor-BNI followed immediately by U50 microinjection were then unilaterally microinjected in the BST ($n = 6$ each) or MPA ($n = 6$ each). The drugs were allowed 2 min for distribution. The experimental period then entailed measurement of CV and RSNA parameters, and collection of urine for 60 min (six consecutive 10-min periods). Urine volume was determined by weight of the vial pre- and posturine output. The urinary sodium and potassium concentration were analyzed by a flame photometer (Jenway PFP7 Flame photometer, Burlington, NJ). To ensure precision, the saline vehicle containing fluorescence beads was microinjected at the end of the experiment in order to determine the injection site. Because of diffusion of beads/drug preparations, the microinjection site was determined by the location of intense fluorescence. Only injection sites within the anterolateral BST or MPA regions were used for data analysis.

Histological processing

At the end of the microinjection study, anesthetized rats were given hexamethonium and euthanized by overdose of the anesthetic followed by decapitation. The brain was then removed and postfixed with 4% paraformaldehyde at 4°C for at least 3 days and moved to 20% sucrose for another 2–3 days. The brains were frozen and cut in 40-μm coronal sections using a cryostat microtome (Avantik QS11, Springfield, NJ). All sections were collected, mounted to glass slides coated in gel alcohol, coverslipped, and allowed to dry. The microinjections sites were

identified microscopically using a fluorescence microscope (Olympus BX41, Center Valley, PA) and the atlas of Paxinos and Watson (2007) as a reference.

Drugs

The drugs used in this study, alpha-chloralose, urethane, inactin, U50, norbinaltorphimine, and hexamethonium, were all purchased from Sigma Aldrich. Sodium chloride 0.9% was obtained from Fisher Scientific (Pittsburgh, PA). Isoflurane (ISOTHESIA) was purchased through the University of Texas from Henry Schein Animal Health (Dublin, OH).

Data analysis

All data are expressed as mean $\pm$ SEM. Data were statistically analyzed using repeated measures analysis of variance (ANOVA) for the change in parameters at different time points after injection of drug as compared with respective control period and a Dunnett's post hoc test for pairwise comparisons among the means. Using the time and the treatment as a repeated factor, a two-way ANOVA was also performed followed by a Bonferroni posttest in order to determine differences occurring between two or more treatment groups at equivalent time periods. In each case, statistical significance was defined as $P < 0.05$ (Prism, ver. 5; Graph Pad software, San Diego, CA).

Results

The CV, renal excretory, and renal sympathetic nerve responses produced by unilateral microinjection of isotonic saline vehicle ($n = 6$, 60 nL), U50 alone ($n = 6$, 100 ng/60 nL), or nor-BNI followed by U50 ($n = 6$) into the anterolateral BST are shown in Figure 1. Unilateral microinjection of U50 into the anterolateral BST evoked significant increases in urine flow rate (V) without increases in HR, mean arterial pressure (MAP), RSNA, or sodium excretion rate (UNaV) relative to its control period. As compared to its respective control levels (V, 25.6 $\pm$ 4.7 μL/min), microinjection of U50 produced a significant increase in urine output starting at 20 min, peaking at 30 min (V, 84.8 $\pm$ 14 μL/min), and returning close to baseline at 60 min. In addition, the kappa-mediated diuretic effect was also significantly different when compared to isotonic saline or nor-BNI plus U50, starting at 20 min and reaching the highest level of statistical significance at 30 and 40 min. The effects of U50 were also significantly different compared to saline vehicle at 50 min and nor-BNI at 60 min. No significant changes in measured parameters were observed in rats microinjected
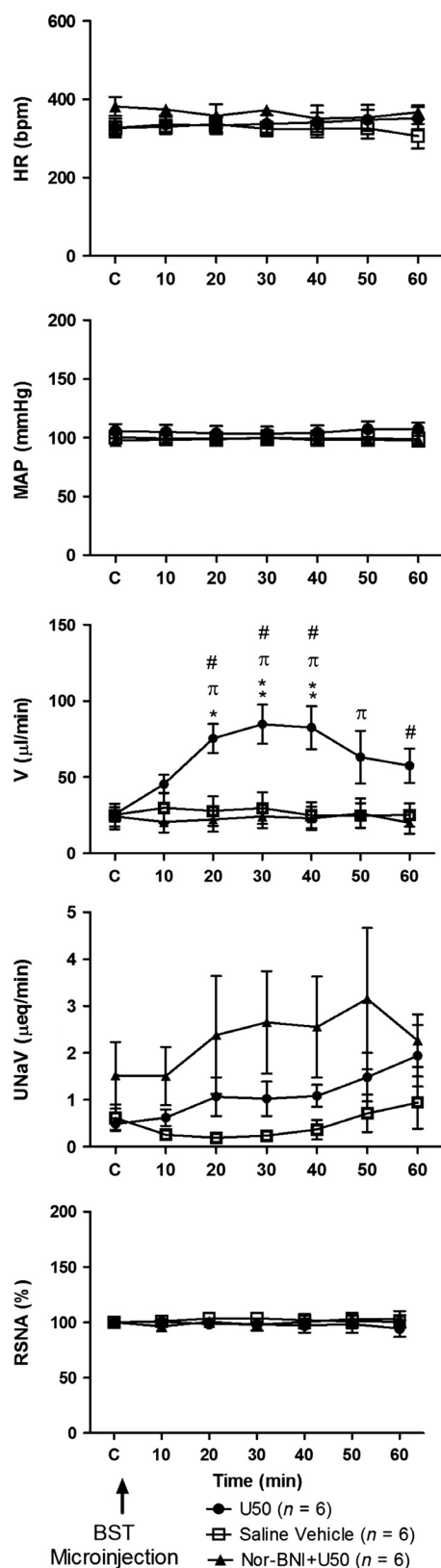
Figure 1. Cardiovascular, renal and renal sympathetic nerve responses produced by unilateral microinjection of U50 (•; n= 6), isotonic saline vehicle (□; n= 6), or nor-BNI plus U50 (▲; n= 6) into the BST. Values are expressed as the mean ± SEM HR, heart rate; MAP, mean arterial pressure; V, urine flow rate; UNaV, urinary sodium excretion; RSNA, renal sympathetic nerve activity. * and ** denotes significant different ($P < 0.05$ and $P < 0.01$, respectively) from respective control period. π denotes significant difference ($P < 0.05$ or greater) between U50 and saline vehicle group over at equivalent time points. # denotes significant difference ($P < 0.05$ or greater) between U50 and nor-BNI plus U50 group at equivalent time points. F value = 35.42; Df1=2; Df2=105.

with isotonic saline or nor-BNI plus U50 as compared to their respective controls. Pretreatment with nor-BNI abolished the diuretic effect and appeared to have a small natriuretic effect. However, this did not reach statistical significance as compared to its control period or other groups.

Figure 2 shows the changes in MAP, HR, V, UNaV, and RSNA produced by unilateral microinjection of U50 ($n = 6$), isotonic saline ($n = 6$), or nor-BNI plus U50 ($n = 6$) into the MPA. Microinjection of U50 into the MPA produced no significant changes in CV, diuretic, and natriuretic parameters. In contrast, U50 microinjection evoked significant increases in RSNA compared to baseline control values from time points 20–60 min. This change in RSNA produced by U50 also differed significantly from that in rats microinjected with isotonic saline or nor-BNI plus U50 over the same time periods. Similar to BST microinjections, isotonic saline vehicle failed to evoke significant changes to any measured parameter. As we observed with microinjections into the BST, injection of nor-BNI plus U50 into the MPA was associated with a nonsignificant trend toward increase in UNaV.

To further corroborate our pharmacological data supporting a role for central KOR-mediated increase in V and RSNA in the BST and MPA, we measured the brain KOR expression in healthy SD rats as shown in Figure 3. The KOR was present not only in the PVN and SON as previously demonstrated (Mansour et al. 1994, 1996) but also in the MPA, anterior (A-BST), and dorsal (D-BST) portions of the BST. There was no statistically significant difference in the expression of KOR among the sites. Figure 4 illustrates the histologically identified sites into which U50 was microinjected into the anterolateral BST and MPA. Although not shown, saline vehicle and nor-BNI injections were also confined to the anterolateral BST or MPA.

Discussion

Data from past studies indicate that the ICV injection of U50 produces a marked free water diuresis with a concurrent increase in RSNA in both anesthetized and conscious
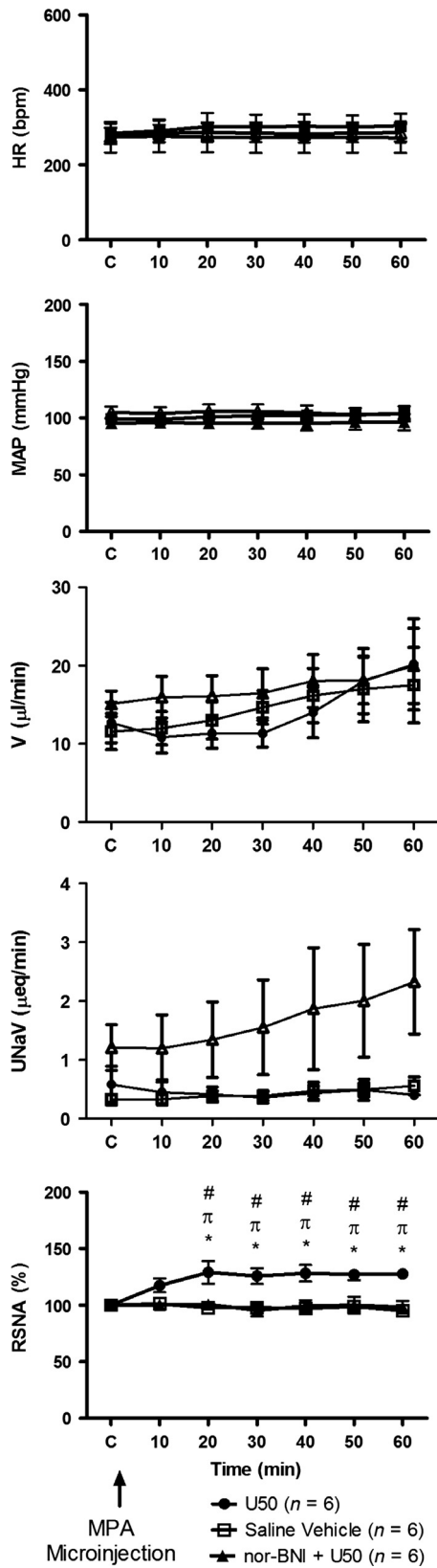
Figure 2. Cardiovascular, renal and RSNA responses produced by microinjection of U50 (•; 5 μl, n = 6), isotonic saline vehicle (□; n= 6), or nor-BNI plus U50 (▲; n= 6) into the MPA of anesthetized rats. Values represent the mean ± SEM. HR, heart rate; MAP, mean arterial pressure; V, urine flow rate; UNaV, urinary sodium excretion; RSNA, renal sympathetic nerve activity. * denotes significant different (P < 0.05) from respective control period.*; P < 0.05, significantly different from respective control period. π, # denotes significant difference (P < 0.001) between U50 and saline or nor-BNI plus U50 groups, respectively, at equivalent time points. F value = 56.30; Df1=2; Df2=105.
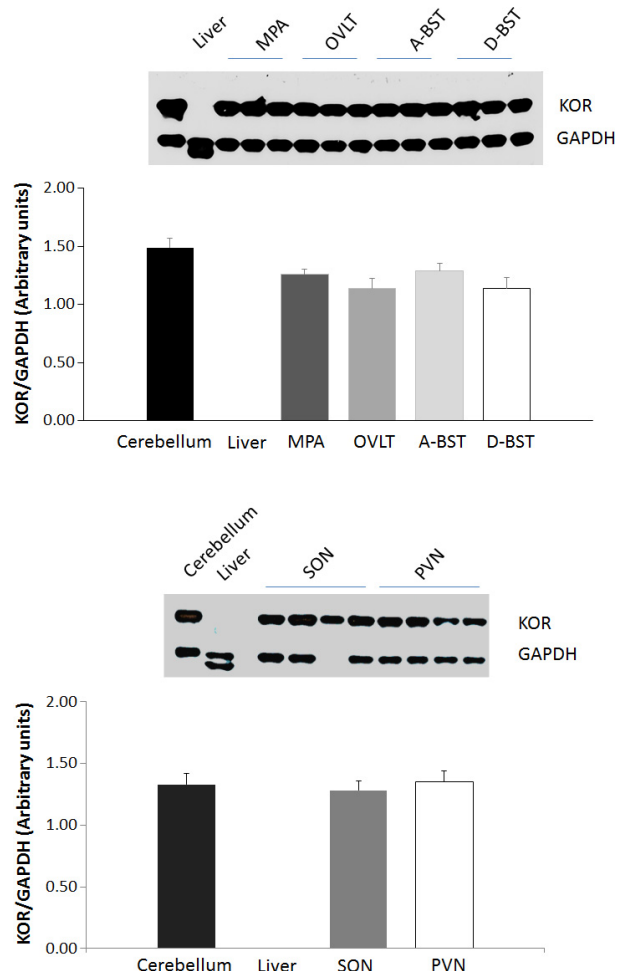
Figure 3. Representative Western blot analysis and corresponding immunolabeling of the kappa opioid receptor (KOR) protein in selected forebrain regions of naïve rats. Values represent the mean ± SEM. Normalized with glyceraldehyde-3-phosphate dehydrogenase (GAPDH), Western blot analysis revealed the kappa opioid receptor 40kD protein band in brain regions from naïve animals. SON, supraoptic nucleus; PVN, paraventricular nucleus of the hypothalamus; MPA, medial preoptic area, A-BST; anterior region of the BST, B-BST; dorsal region of the BST.
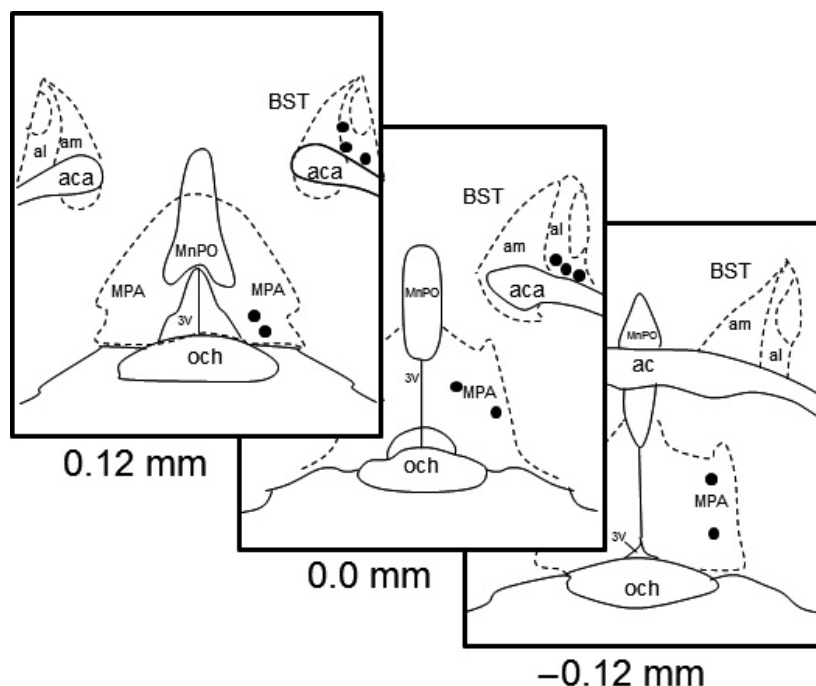
Figure 4. Schematic coronal sections adapted from the atlas of Paxinos and Watson, demonstrating microinjection sites into which the selective kappa opioid receptor agonist, U-50488H (100 ng/60 nl), was microinjected into the anterolateral BST or MPA. Microinjections are approximates based on the fluorescence intensity. Numbers indicate the distance in millimeters from bregma. och, optic chiasm; 3v, third ventricle; MnPO, median preoptic nucleus; aca, anterior commissure; am, anteromedial BST; al, anterolateral BST.

rats (Kapusta et al. 1989; Kapusta 1995; Gottlieb et al. 2005a). However, the CNS sites via which KOR modulate these responses are yet to be fully characterized. The results presented in our studies demonstrate that the KOR is present in the LT and that activation of KOR at anterolateral BST and MPA evokes different modulatory effects on urine excretion rate and RSNA. These changes occurred without concurrent changes in MAP, HR, and UNaV. These data suggest a novel pathway by which activation of central KOR can modulate water and renal sympathetic nerve function.

The BST is thought to serve as a relay center between limbic cognitive centers and nuclei involved in the processing of reward, stress, and anxiety (Poulin et al. 2009). Moreover, it is divided into several regions and projects to the hypothalamic sites involved in production and secretion of AVP (Dong and Swanson 2006a; Crestani et al. 2013). Therefore, the BST seems to play an important role in the integration of physiological and behavioral responses associated with autonomic and neuroendocrine functions. Our studies demonstrate that unilateral microinjection of U50 into the anterolateral BST significantly increases urine flow rate as compared to baseline control. This increase in urine was also significantly different from rats microinjected with saline vehicle. Pretreatment with the selective KOR antagonist, nor-BNI, abolished the

diuretic response evoked by U50. Although this increase in urine flow rate was not equivalent in magnitude to ICV administration in anesthetized (U50; 10 μg/5 μL) rats as previously reported (Gottlieb et al. 2005b), it was similar in duration and peak time. Furthermore, microinjection of a similar dose of U50 (100 ng/60 nL) into the BST evoked a diuretic response similar to that previously reported by us after bilateral U50 microinjection into the magnocellular PVN, (Gottlieb et al. 2005b). Although a different anesthetic cocktail was used in this study, the KOR-mediated diuretic effect observed was similar in duration and trend to those observed anesthetized and conscious studies previously mentioned. In this study, the anesthetic used during the experimental protocol was urethane–alpha-chloralose, which has been used consistently in electrophysiology studies measuring CV and sympathetic function (Cardoso et al. 2009; Pedrino et al. 2013; Bardgett et al. 2014). This anesthesia cocktail did not appear to modulate AVP secretion as evoked by certain barbiturates and ketamine/xylazine (Walter et al. 1989; Gottlieb et al. 2005b). Although not shown in this manuscript, ICV injection of U50 evoked similar magnitude and duration of action in this anesthetized model.

Whole animal studies support the hypothesis that KOR produce diuresis by inhibiting central AVP secretion and that this decrease was paralleled by an increase in urine

flow rate (Slizgi and Ludens 1982, 1986; Leander et al. 1985). In addition, in vivo and in vitro studies demonstrated that activation of KOR can suppress the phasic firing patterns of AVP magnocellular neurons in the SON, which results in the decrease in AVP secretion (Inenaga et al. 1994; Rossi and Brooks 1996; Brown et al. 1998, 2000, 2006). Furthermore, administration of nor-BNI increased the burst duration and firing frequency of the phasic vasopressinergic neurons (Brown et al. 1998). Although plasma levels of AVP were not measured in this study, the consensus is that the predominant mechanism by which KOR produce diuresis is via a central inhibition of AVP secretion. This is the first study to demonstrate that activation of KOR receptors outside the hypothalamic sites (PVN and SON) may also evoke a diuretic effect potentially through inhibition of AVP secretion. Although more experiments are necessary to determine the pathway and mechanism involved, one can postulate that BST neurons may play a tonic role in stimulating vasopressin secretion at the level of the PVN and/or SON, in this anesthetized model. Thus, activation of KOR, which are typically inhibitory (Connor and Christie 1999), suppresses this pathway, resulting in a reduction of plasma AVP and concurrent increase in urine flow. This hypothesis is supported by studies demonstrating the existence of a neuronal projection from the BST to magnocellular neurons in the PVN and SON (Crestani et al. 2013) and other studies suggesting that KOR activation decreases plasma AVP secretion (Oiso et al. 1988; Brooks et al. 1993; Kapusta 1995; Rossi and Brooks 1996).

ICV administration of U50 has been demonstrated to produce a decrease in sodium excretion rate with a concurrent increase in RSNA (Kapusta and Obih 1993; Kapusta 1995; Gottlieb and Kapusta 2005). In an attempt to identify other potential sites involved in the KOR-mediated effects on RSNA, we microinjected U50 into the MPA. The MPA, which lies near the organum vasculosum of the LT, have been implicated in the modulation of sympathetic nerve activity (Hubschle et al. 1998; Sly et al. 1999). Microinjection of U50 into MPA did not increase the measured CV or renal parameters, but evoked a significant increase in RSNA. ICV injection of U50 in conscious rats was reported to produce an increase in RSNA that peaks at 30 min and begins returning to baseline values within 50 min (Kapusta and Obih 1993). Similarly, we previously reported results of experiments in a ketamine/xylazine anesthetized model, in which increases in RSNA induced by U50 were significant by 30 min and remained significantly elevated ($\approx$50%) above baseline for at least another 50 min (Gottlieb et al. 2005b). In this study, unilateral microinjection of U50 into the MPA evoked a similar pattern, but at a lower magnitude ($\approx$30%) of increase. Similar to the results observed by

microinjection of U50 into the BST, MPA injections did not evoke any significant changes to urinary sodium excretion rate. This is interesting since increases in RSNA have been previously been reported to be associated with a KOR-mediated antinatriuretic effect in heathy rats (Kapusta and Obih 1993). However, in our experiments, we did not detect a decrease in UNaV. The differences observed in antinatriuresis and RSNA activity in this study and previous reports maybe attributed to the use of smaller dose than ICV and the unilateral administration of U50 compared to other methods used in peer-reviewed studies. It is also possible that the lack of antinatriuretic effect may be caused by the anesthesia used in this protocol. Although the increase in RSNA can influence UNaV, under certain conditions, it has also been shown to be independent of the renal nerves (Kapusta et al. 1989). Furthermore, while other CNS regions may contribute to the antinatriuretic effects of U50, our data provide evidence that activation of KOR in the MPA increases RSNA. The western blot data demonstrate the presence of the receptor in these sites and along with the antagonist data, support our conclusion that the responses observed are selective to the activation of KOR.

In conclusion, microinjection of the kappa opioid agonist into the anterolateral BST and MPA evoke selective changes in urine flow rate and RSNA. Thus, this study identifies two regions within the LT that may be involved in the opioid-mediated control of electrolyte and water homeostasis through kappa receptors. This is the first study demonstrating that activation of KOR at a site other than that of magnocellular AVP neurons present in the PVN or SON can evoke increases in urine output. The results presented in our studies demonstrate a novel pathway for the kappa opioid-mediated diuretic effect in the BST and increased sympathetic outflow to the kidneys. These results provide a rationale for future studies aimed at elucidating the mechanism underlying this response. These results provide new information concerning the role of kappa opioids in the regulation of body fluid homeostasis, which may lead to the development of novel therapeutic approaches for diseases that evolves fluid overload and hyponatremia.

Acknowledgements

Author Contributions

conducted the experiments. Fortepiani and Gottlieb performed the data analysis. Franklin, Fortepiani, Nguyen, Rangel, Strong, and Gottlieb wrote or contributed to the writing of the manuscript.

Disclosures

None declared.

References

Bardgett ME, Sharpe AL, Toney GM (2014). Activation of corticotropin releasing factor receptors in the rostral ventrolateral medulla is required for glucose-induced sympathoexcitation. Am J Physiol Endocrinol Metab 307(10): E944–953.

Bealer SL, Johnson AK (1979). Sodium consumption following lesions surrounding the anteroventral third ventricle. Brain Res Bull 4: 287–290.

Boudaba C, Szabo K, Tasker JG (1996). Physiological mapping of local inhibitory inputs to the hypothalamic paraventricular nucleus. J Neurosci 16: 7151–7160.

Brody MJ, Johnson AK (1980). Role of the anteroventral third ventricle region in fluid and electrolyte balance, arterial pressure regulation and hypertension. Front Neuroendocrinol 6: 249–285.

Brooks DP, Giardina G, Gellai M, Dondio G, Edwards RM, Petrone G, et al. (1993). Opiate receptors within the blood brain barrier mediate k agonist-induced water diuresis. J Pharmacol Exp Therap 266: 164–171.

Brown CH, Ludwig M, Leng G (1998). kappa-opioid regulation of neuronal activity in the rat supraoptic nucleus in vivo. J Neurosci 18: 9480–9488.

Brown CH, Ghamari-Langroudi M, Leng G, Bourque CW (1999). Kappa-opioid receptor activation inhibits post-spike depolarizing after-potentials in rat supraoptic nucleus neurones in vitro. J Neuroendocrinol 11: 825–828.

Brown CH, Russell JA, Leng G (2000). Opioid modulation of magnocellular neurosecretory cell activity. Neurosci Res 36: 97–120.

Brown CH, Leng G, Ludwig M, Bourque CW (2006). Endogenous activation of supraoptic nucleus kappa-opioid receptors terminates spontaneous phasic bursts in rat magnocellular neurosecretory cells. J Neurophysiol 95: 3235–3244.

Cardoso LM, Colombari DS, Menani JV, Toney GM, Chianca Jr DA, Colombari E (2009). Cardiovascular responses to hydrogen peroxide into the nucleus tractus solitarius. Am J Physiol Regul Integr Comp Physiol 297: R462–R469.

Connor M, Christie MD (1999). Opioid receptor signalling mechanisms. Clin Exp Pharmacol Physiol 26: 493–499.

Conway EL, Maccarrone C, Verberne AJ, Louis WJ (1987). Dynorphin(1-8) immunoreactivity in brainstem and hypothalamic nuclei of normotensive and age-matched hypertensive rat strains. Clin Exp Hypertens A 9: 109–124.

Crestani CC, Alves FH, Gomes FV, Resstel LB, Correa FM, Herman JP (2013). Mechanisms in the bed nucleus of the stria terminalis involved in control of autonomic and neuroendocrine functions: a review. Curr Neuropharmacol 11: 141–159.

Diez-Guerra FJ, Augood S, Emson PC, Dyer RG (1987). Opioid peptides inhibit the release of noradrenaline from slices of rat medial preoptic area. Exp Brain Res 66: 378–384.

Dong HW, Swanson LW (2006a). Projections from bed nuclei of the stria terminalis, anteromedial area: cerebral hemisphere integration of neuroendocrine, autonomic, and behavioral aspects of energy balance. J Comp Neurol 494: 142–178.

Dong HW, Swanson LW (2006b). Projections from bed nuclei of the stria terminalis, dorsomedial nucleus: implications for cerebral hemisphere integration of neuroendocrine, autonomic, and drinking responses. J Comp Neurol 494: 75–107.

Dong HW, Petrovich GD, Swanson LW (2001). Topography of projections from amygdala to bed nuclei of the stria terminalis. Brain Res Brain Res Rev 38: 192–246.

Gaykema RP, Chen CC, Goehler LE (2007). Organization of immune-responsive medullary projections to the bed nucleus of the stria terminalis, central amygdala, and paraventricular nucleus of the hypothalamus: evidence for parallel viscerosensory pathways in the rat brain. Brain Res 1130: 130–145.

Gottlieb HB, Kapusta DR (2005). Endogenous central kappa-opioid systems augment renal sympathetic nerve activity to maximally retain urinary sodium during hypotonic saline volume expansion. Am J Physiol Regul Integr Comp Physiol 289: R1289–R1296.

Gottlieb HB, Ji LL, Jones H, Penny ML, Fleming T, Cunningham JT (2005a). Differential effects of water and saline intake on water deprivation induced c-Fos staining in the rat. Am J Physiol Regul Integr Comp Physiol 290(5): R1251–1261.

Gottlieb HB, Varner KJ, Kenigs VA, Cabral AM, Kapusta DR (2005b). Differential cardiovascular and renal responses produced by microinjection of the {kappa}-opioid U-50488H [(trans-3,4-dichloro-N-methyl-N-[2-(1-pyrrolidinyl) cyclohexyl]-benzene-ace tamide) methane sulfonate] into subregions of the paraventricular nucleus. J Pharmacol Exp Ther 312: 678–685.

Grob M, Trottier JF, Drolet G, Mouginot D (2003). Characterization of the neurochemical content of neuronal populations of the lamina terminalis activated by acute hydromineral challenge. Neuroscience 122: 247–257.

Hubschle T, McKinley MJ, Oldfield BJ (1998). Efferent connections of the lamina terminalis, the preoptic area and the insular cortex to submandibular and sublingual gland of the rat traced with pseudorabies virus. Brain Res 806: 219–231.

Hunt JL, Zaretsky DV, Sarkar S, Dimicco JA (2010). Dorsomedial hypothalamus mediates autonomic, neuroendocrine, and locomotor responses evoked from the medial preoptic area. Am J Physiol Regul Integr Comp Physiol 298: R130–R140.

Inenaga K, Nagatomo T, Nakao K, Yanaihara N, Yamashita H (1994). Kappa-selective agonists postsynaptic potentials and calcium components of action potentials in the supraoptic nucleus of rat hypothalamus in vitro. Neuroscience 58: 331–340.

Kapusta DR (1995). Opioid mechanisms controlling renal function. Clin Exp Pharmacol Physiol 22: 891–902.

Kapusta DR, Obih JC (1993). Central kappa opioid receptor-evoked changes in renal function in conscious rats: participation of renal nerves. J Pharmacol Exp Ther 267: 197–204.

Kapusta DR, Jones SY, DiBona GF (1989). Role of renal nerves in excretory responses to administration of kappa agonists in conscious spontaneously hypertensive rats. J Pharmacol Exp Ther 251: 230–237.

Kawano H, Masuko S (2000). Beta-endorphin-, adrenocorticotrophic hormone- and neuropeptide γ-containing projection fibers from the arcuate hypothalamic nucleus make synaptic contacts on to nucleus preopticus medianus neurons projecting to the paraventricular hypothalamic nucleus in the rat. Neuroscience 98: 555–565.

Leander JD, Zerbe RL, Hart JC (1985). Diuresis and suppression of vasopressin by kappa opioids: comparison with mu and delta opioids and clonidine. J Pharmacol Exp Ther 234: 463–469.

Leander JD, Hart JC, Zerbe RL (1987). Kappa agonist-induced diuresis: evidence for stereoselectivity, strain differences, independence of hydration variables and a result of decreased plasma vasopressin levels. J Pharmacol Exp Ther 242: 33–39.

Llewellyn T, Zheng H, Liu X, Xu B, Patel KP (2012). Median preoptic nucleus and subfornical organ drive renal sympathetic nerve activity via a glutamatergic mechanism within the paraventricular nucleus. Am J Physiol Regul Integr Comp Physiol 302: R424–R432.

Mansour A, Fox CA, Meng F, Akil H, Watson SJ (1994). Kappa 1 receptor mRNA distribution in the rat CNS: comparison to kappa receptor binding and prodynorphin mRNA. Mol Cell Neurosci 5: 124–144.

Mansour A, Burke S, Pavlic RJ, Akil H, Watson SJ (1996). Immunohistochemical localization of the cloned kappa 1 receptor in the rat CNS and pituitary. Neuroscience 71: 671–690.

Maolood N, Meister B (2008). Dynorphin in pro-opiomelanocortin neurons of the hypothalamic arcuate nucleus. Neuroscience 154: 1121–1131.

McKinley MJ, Bicknell RJ, Hards D, McAllen RM, Vivas L, Weisinger RS, et al. (1992). Efferent neural pathways of the lamina terminalis subserving osmoregulation. Prog Brain Res 91: 395–402.

McKinley MJ, Allen AM, May CN, McAllen RM, Oldfield BJ, Sly D, et al. (2001). Neural pathways from the lamina terminalis influencing cardiovascular and body fluid homeostasis. Clin Exp Pharmacol Physiol 28: 990–992.

McKinley MJ, Mathai ML, McAllen RM, McClear RC, Miselis RR, Pennington GL, et al. (2004). Vasopressin secretion: osmotic and hormonal regulation by the lamina terminalis. J Neuroendocrinol 16: 340–347.

Morrison SF (2011). 2010 Carl Ludwig Distinguished Lectureship of the APS Neural Control and Autonomic Regulation Section: Central neural pathways for thermoregulatory cold defense. J Appl Physiol 110: 1137–1149.

Oiso Y, Iwasaki Y, Kondo K, Takatsuki K, Tomita A (1988). Effect of the opioid kappa-receptor agonist U50488H on the secretion of arginine vasopressin. Study on the mechanism of U50488H-induced diuresis. Neuroendocrinology 48: 658–662.

Paxinos G, Watson C (2007). The rat brain in stereotaxic coordinates. 6th Edition. Academic Press, Elsevier.

Pedrino GR, Calderon AS, Andrade MA, Cravo SL, Toney GM (2013). Discharge of RVLM vasomotor neurons is not increased in anesthetized angiotensin II-salt hypertensive rats. Am J Physiol Heart Circ Physiol 305: H1781–H1789.

Poulin JF, Arbour D, Laforest S, Drolet G (2009). Neuroanatomical characterization of endogenous opioids in the bed nucleus of the stria terminalis. Prog Neuropsychopharmacol Biol Psychiatry 33: 1356–1365.

Roland BL, Sawchenko PE (1993). Local origins of some GABAergic projections to the paraventricular and supraoptic nuclei of the hypothalamus in the rat. J Comp Neurol 332: 123–143.

Rossi NF, Brooks DP (1996). kappa-Opioid agonist inhibition of osmotically induced AVP release: preferential action at hypothalamic sites. Am J Physiol 270(2 Pt. 1): E367–E372.

Sawchenko PE, Swanson LW (1983). The organization of forebrain afferents to the paraventricular and supraoptic nuclei of the rat. J Comp Neurol 218: 121–144.

Slizgi GR, Ludens JH (1982). Studies on the nature and mechanism of the diuretic activity of the opioid analgesic ethylketocyclazocine. J Pharmacol Exp Ther 220: 585–591.

Slizgi GR, Ludens JH (1986). Role of ADH in ethylketocyclazocine-induced diuresis: studies in the Brattleboro rat. Life Sci 38: 2437–2440.

Sly DJ, Colvill L, McKinley MJ, Oldfield BJ (1999). Identification of neural projections from the forebrain to the kidney, using the virus pseudorabies. J Auton Nerv Syst 77: 73–82.

Walter SJ, Zewde T, Shirley DG (1989). The effect of anaesthesia and standard clearance procedures on renal function in the rat. Q J Exp Physiol 74: 805–812.

Zardetto-Smith AM, Thunhorst RL, Cicha MZ, Johnson AK (1993). Afferent signaling and forebrain mechanisms in the behavioral control of extracellular fluid volume. Ann N Y Acad Sci 689: 161–176.